nature medicine

Supplementary information

https://doi.org/10.1038/s41591-024-03213-1

Unidirectional association of clonal hematopoiesis with atherosclerosis development

In the format provided by the authors and unedited

Supplementary Table 1. Candidate driver genes and variants queried for the detection of clonal hematopoiesis.

Gene	RefSeq	Candidate CH variants
ASXL1	NM_015338.6	Frameshift/nonsense/splice-site in exons 12-13
ATM	NM_000051.4	Frameshift/nonsense/splice-site, missense in P1054H, A1309T, p.1940–2566 (FAT domain), p.2712-2962 (PI3K/PI4K domain)
BCL11B	NM_138576.4	Missense in p.221–251, p.427–454, p.455–482, p.796–823, p.824–853, p.854–884 (Zn finger domains)
BCOR	NM_001123385.2	Frameshift/nonsense/splice-site
BCORL1	NM_021946.5	Frameshift/nonsense/splice-site
BIRC3	NM_001165.5	Frameshift/nonsense/splice-site
BRAF	NM_004333.6	G464E, G464V, G466E, G466V, G469R, G469E, G469A, G469V, V471F, V472S, L485W, N581S, I582M, I592M, I592V, D594N, D594G, D594V, D594E, F595L, F595S, G596R, L597V, L597S, L597Q, L597R, A598V, V600M, V600L, V600K, V600R, V600E, V600A, V600G, V600D, K601E, K601N, R603*, W604R, W604G, S605G, S605F, S605N, G606E, G606A, G606V, H608R, H608L, G615R, S616P, S616F, L618S, L618W
BRCC3	NM_024332.4	Frameshift/nonsense/splice-site
CARD11	NM_032415.7	Missense in exons 4-8 (CC domain), E626
CBL	NM_005188.4	Missense in p.352-p.420 (RING finger and linker region)
CD58	NM_001779.3	Frameshift/nonsense/splice site
CD79B	NM_000626.4	Missense in p.196
CNOT3	NM_014516.4	Frameshift/nonsense/splice-site, missense in E20K, p.661 – 753 (repressor domain)
CREBBP	NM_004380.3	Frameshift/nonsense/splice-site, D1435E, R1446L, R1446H, R1446C, Y1450C, P1476R, Y1482H, H1487Y, W1502C, Y1503D, Y1503H, Y1503F, S1680del
CUX1	NM_181552.4	Frameshift/nonsense
DDX3X	NM_001356.5	Frameshift/nonsense
DNMT3A	NM_175629.2	Frameshift/nonsense/splice-site, missense in F290I, F290C, p.292 – 350 (PWWP domain),Y365C, R366P, R366H, R366G, R366L, A368T, A368V, R379H, R379C, I407T, I407N, I407S, A410T, F414L, F414S, F414C, A462V, K468R, E469V, E477K, p.482 – 614 (ADD domain), R631G, p.634 – 912 (MTase domain), F732del, F752del
EZH2	NM_004456.5	Frameshift/nonsense/splice-site, Q62R, N102S, F145S, F145C, F145Y, F145L, G159R, E173D, Y292C, P493S, R502Q, R566H, T573I, p.612 – 727 (SET domain), E745K
FLT3	NM_004119.3	V579A, V592A, V592I, F594L, FY590-591GD, D835Y, D835H, D835E, del835
GNAS	NM_080425.4	R844S, R844C, R844H, R844L, Q870K, Q870R, Q870L, Q870H, R1017C
GNB1	NM_002074.5	K57N, K57M, K57E, K57T, I80T, I80N
IDH2	NM_002168.4	R140W, R140Q, R140L, R140G, R172W, R172G, R172K, R172T, R172M, R172N, R172S
IKZF1	NM_006060.6	Frameshift/nonsense
JAK2	NM_004972.4	N533D, N533Y, N533S, H538R, K539E, K539L, I540T, I540V, V617F, R683S, R683G, del/ins537-539L, del/ins538-539L, del/ins540-543MK, del/ins540-544MK, del/ins541-543K, del542-543, del543-544, ins546-547
KDM6A	NM_021140.4	Frameshift/nonsense/splice-site, missense in p. 93-385 (TPR domain), p.1095-1258 (JmjC domain)
KIT	NM_000222.3	Missense in p.410-512, V559A, V559D, V559G, V559I, V560D, V560A, V560G, V560E, E561K, , P627L, P627T, R634W, K642E, K642Q, V654A, V654E, H697Y, H697D, E761D, K807R, D816H, D816Y, D816F, D816I, D816V, D816H, ins503, del560, del579, del551-559
KMT2D	NM_003482.4	Frameshift/ nonsense
KRAS	NM_033360.4	G12D, G12A, G12E, G12V, G12R, G13D, G13C, G13Y, G13F, G13R, G13A, G13V, G13E, V14I, A18D, T58I, G60D, G60A, G60V, Q61K, Q61E, Q61P, Q61R, Q61L, Q61H, K117E, K117N, K117R, A146T, A146P, A146V
LUC7L2	NM_016019.5	Frameshift/nonsense/splice-site
MPL	NM_005373.3	S505G, S505N, S505C, L510P, del513, W515A, W515R, W515K, W515S, W515L, A519T, A519V, Y591D, Y591H, W515-518KT, Y591D, R592Q
MYD88	NM_001172567.2	Missense in p.159 – 293 (TIR domain)
NOTCH1	NM_017617.5	Frameshift/nonsense in exon 34 (TAD and PEST domains)
NOTCH2	NM_024408.4	Frameshift/nonsense in exon 34 (TAD and PEST domains)

NRAS	NM_002524.5	G12S, G12R, G12C, G12N, G12P, G12Y, G12D, G12A, G12V, G12E, G13S, G13R, G13C, G13N, G13P, G13Y, G13D, G13A, G13V, G13E, G60E, G60R, Q61R, Q61L, Q61K, Q61P, Q61H, Q61Q, Y64D
PPM1D	NM_003620.4	Frameshift/nonsense in exons 5-6
PRDM1	NM_001198.4	Frameshift/nonsense, missense in p.84-201 (SET domain)
PRPF40B	NM_001031698.3	Frameshift/nonsense/splice-site, P15H, M58I, P405L, P562S
PTPN11	NM_002834.5	G60V, G60R, G60A, D61Y, D61V, D61G, Y63C, E69K, E69G, E69D, E69Q, F71L, F71K, A72T, A72V, A72D, T73I, E76K, E76Q, E76M, E76A, E76G, E139G, E139D, N308D, N308T, N339S, P491L, S502P, S502A, S502L, G503V, G503G, G503A, G503E, Q506P, T507A, T507K
RAD21	NM_006265.3	Frameshift/nonsense/splice-site, R65Q, H208R, Q474R
SETD2	NM_014159.7	Frameshift/nonsense. Missense in V1190M, p.1494-1548 (AWS domain), p.1550-1667 (SET domain), p.1674-1690 (post SET domain), p.2389-2422 (WW domain)
SETDB1	NM_001145415.2	Frameshift/nonsense, missense in p.594 – 665 (MBD domain), K715E, p.803 – 1266 (SET domain)
SF1	NM_004630.4	Frameshift/nonsense/splice-site, T454M, Y476C, A508G
SF3B1	NM_012433.4	G347V, R387W, R387Q, E592K, E622D, Y623C, R625L, R625C, R625G, H662Q, H662D, T663I, K666N, K666T, K666E, K666R, K666Q, K700E, V701F, A708T, G740R, G740E, K741N, G742D, A744P, D781G, E783K, R831Q, L833F, E862K, R957Q
SMC3	NM_005445.4	Frameshift/nonsense, R155I, Q367E, D392V, K571R, R661P, G662C
SRSF2	NM_003016.4	Y44H, P95H, P95L, P95T, P95R, P95A, P96L, P107H, P95fs
STAT3	NM_139276.3	Missense in p.584-674 (SH2 domain)
SUZ12	NM_015355.4	Frameshift/nonsense
TET2	NM_001127208.3	Frameshift/nonsense/splice-site, missense mutations in p.1129-1312 (Cys-rich domain), p.1312-1936 (DSBH domain)
TNFAIP3	NM_001270508.2	Frameshift/nonsense
TNFRSF14	NM_003820.4	Frameshift/nonsense/splice-site
TP53	NM_000546.6	Frameshift/nonsense/splice-site, S46F, G105C, G105R, G105D, G108S, G108C, R110L, R110C, T118A, T118R, T118I, S127F, S127Y, L130V, L130F, K132Q, K132E, K132W, K132R, K132M, K132N, F134V. F134L, F134S, C135W, C135S, C135F, C135G, C135Y, Q136K, Q136E, Q136P, Q136R, Q136L, Q136H, A138P, A138V, A138A, A138T, T140I, C141R, C141G, C141A, C141Y, C141S, C141F, C141W, V143M, V143A, V143E, L145Q, W146C, W146L, L145R, V147G, P151T, P151A, P151S, P151H, P151R, P152S, P152R, P152L, T155P, T155A, V157F, R158H, R158L, A159V, A159P, A159S, A159D, A161T, A161D, Y163N, Y163H, Y163D, Y163S, Y163C, K164E, K164M, K164N, K164P, H168Y, H168P, H168R, H168L, H168Q, M169I, M169T, M169V, E171K, E171Q, E171G, E171A, E171V, E171D, V172D, V173M, V173L, V173G, R174W, R175G, R175C, R175H, C176R, C176G, C176Y, C176F, C176S, P177R, P177R, P177L, H178D, H178P, H178Q, H179Y, H179R, H179Q, R181C, R181Y, D186G, G187S, P190L, P190T, H193N, H193P, H193L, H193R, L194F, L194R, I195F, I195N, I195T, R196P, V197L, G199V, Y205N, Y205C, Y205H, D208V, R213Q, R213P, R213L, R213Q, H214D, H214R, S215G, S215I, S215R, V216M, V217G, Y220N, Y220H, Y220S, Y220C, E224D, I232F, I232N, I232T, I232S, Y234N, Y234H, Y234S, Y234C, Y236N, Y236H, Y236C, M237V, M237K, M237I, C238R, C238G, C238Y, C238W, N239T, N239S, S241Y, S241C, S241F, C242G, C242Y, C242S, C242F, G244S, G244C, G244D, G245S, G245R, G245C, G245D, G245A, G245V, G245S, M246V, M246K, M246R, M246I, N247I, R248W, R248G, R248Q, R249G, R249W, R249T, R249M, P250L, I251N, L252P, I254S, I255F, I255N, I255S, L257Q, L257P, E258K, E258Q, D259Y, S261T, G262D, G262V, L265P, G266R, G266E, G266V, R267W, R267Q, R267P, E271K, V272M, V272L, R273S, R273G, R273C, R273H, R273P, R273L, V274F, V274D, V274A, V274G, V274L, C275Y, C275S, C275F, A276P, C277F, C277Y, P278T, P278A, P278S, P278H, P278R, P278L, G279E, R280G, R280K, R280T, R280I, R280S, D281N, D281H, D281Y, D281G, D281E, R282G, R282W, R282Q, R282P, E285K, E285V, E286G, E286V, E286K, K320N, L330R, G334V, R337C, R337L, R337H, A347T, L348F, T377P
U2AF1	NM_006758.3	D14G, S34F, S34Y, R35L, R156H, R156Q, Q157R, Q157P
ZNF318	NM_014345.3	Frameshift/nonsense/splice site
ZRSR2	NM_005089.4	Frameshift/nonsense/splice-site, R126P, E133G, C181F, H191Y, I202N, F239V, F239Y, N261Y, C280R, C302R, C326R, H330R, N382K

Supplementary Table 2. Clonal hematopoiesis-related mutations identified in the study population. We performed deep targeted sequencing to identify somatic mutations in a custom panel of 54 clonal hematopoiesis (CH)-related genes in 3,692 individuals from the PESA cohort. 1,172 CH-related somatic variants were identified in 900 participants in PESA at baseline. Ref. reference; Alt. Alternate; SNV, single nucleotide variant; VAF, variant allele fraction.

Please see Supplementary Table 2 spreadsheet.

Supplementary Table 3. Baseline characteristics of the study population stratified by the presence of CH mutations in *DNMT3A, TET2* and other sequenced genes. Data is expressed as n, %, mean ± SD or median [IQR] when appropriate. P-values were calculated through independent two-tailed t-tests for continuous variables exhibiting a normal distribution, Wilcoxon rank tests for continuous variables with a non-normal distribution and $\chi 2$ tests for categorical variables. BMI, body mass index; CV, cardiovascular; DBP, diastolic blood pressure; HDL-C, high-density lipoprotein cholesterol; LDL-C, low-density lipoprotein cholesterol; SBP, systolic blood pressure; HOMA-IR, Homeostatic Model Assessment for Insulin Resistance; GOT, glutamic-oxaloacetic transaminase; GPT, Glutamic-pyruvic transaminase; GGT, gamma glutamyl transferase.

	No CH (n=2,792)	*DNMT3A* mutations (n=548)	p-value	*TET2* mutations (n=145)	p-value	Other mutated genes	p-value
Age, years	45.0 [42.0 - 49.0]	47.0 [43.8 - 50.2]	<0.001	48.0 [43.0 - 51.0]	<0.001	48.0 [43.0 - 51.0]	<0.001
Men, %	1812 (64.9)	310 (56.6)	<0.001	88 (60.7)	0.345	218 (65.5)	0.886
Dyslipidemia, %	1145 (41.0)	228 (41.6)	0.832	64 (44.1)	0.509	141 (42.3)	0.683
Total cholesterol, mg/dL	200.2 ± 33.3	201.3 ± 33.3	0.461	201.4 ± 33.5	0.670	201.8 ± 32.2	0.400
Low plasma HDL-C, %	904 (32.4)	167 (30.5)	0.411	51 (35.2)	0.542	113 (33.9)	0.609
LDL-C ≥160 mg/dL, %	476 (17.0)	91 (16.6)	0.849	26 (17.9)	0.871	54 (16.2)	0.760
HDL-C, mg/dL	49.0 ± 12.1	50.4 ± 12.9	0.015	49.0 ± 12.1	0.964	49.1 ± 13.1	0.903
LDL-C, mg/dL	132.3 ± 29.7	132.1 ± 28.7	0.882	132.4 ± 31.0	0.973	132.6 ± 28.0	0.879
Plasma triglycerides ≥150 mg/dL, %	303 (10.9)	57 (10.4)	0.813	18 (12.4)	0.652	42 (12.6)	0.381
Triglycerides, mg/dL	79.0 [59.0 - 112.0]	78.0 [60.0 - 111.0]	0.894	83.0 [62.0 - 114.0]	0.194	83.0 [61.0 - 119.0]	0.115
Serum lipoprotein(a), mg/dL	17.6 [6.7 - 43.0]	17.8 [6.7 - 44.2]	0.745	17.5 [6.9 - 44.6]	0.874	18.2 [6.9 - 40.1]	0.839
Hypertension, %	297 (10.6)	69 (12.6)	0.206	22 (15.2)	0.115	51 (15.3)	0.013
SBP, mmHg	116.0 ± 12.2	116.0 ± 12.6	0.961	117.4 ± 13.7	0.204	118.2 ± 13.8	0.004
DBP, mmHg	72.2 ± 9.3	72.8 ± 9.2	0.161	73.6 ± 9.6	0.077	74.0 ± 10.0	0.002
Diabetes mellitus, %	49 (1.8)	12 (2.2)	0.603	6 (4.1)	0.080	4 (1.2)	0.606
Fasting glucose ≥ 100 mg/dL, %	349 (12.5)	69 (12.6)	1.000	29 (20.0)	0.012	53 (15.9)	0.094
Fasting glucose, mg/dL	89.0 [84.0 - 95.0]	89.0 [83.0 - 95.0]	0.587	91.0 [84.0 - 98.0]	0.034	90.0 [85.0 - 97.0]	0.034
Insulin, µU/mL	5.1 [3.6 - 7.4]	5.1 [3.7 - 7.3]	0.418	5.0 [3.7 - 7.4]	0.715	5.3 [3.7 - 7.7]	0.104
HOMA-IR > 2.5, %	266 (9.5)	65 (11.9)	0.111	14 (9.7)	1.000	38 (11.4)	0.318
HOMA-IR	1.1 [0.7 - 1.7]	1.1 [0.8 - 1.7]	0.515	1.1 [0.8 - 1.8]	0.483	1.2 [0.8 - 1.8]	0.081
Hemoglobin A1c, %	5.4 [5.2 - 5.6]	5.4 [5.2 - 5.6]	0.133	5.4 [5.1 - 5.8]	0.228	5.5 [5.2 - 5.7]	0.000
Current smoker , %	542 (19.4)	122 (22.3)	0.143	35 (24.1)	0.198	68 (20.4)	0.717
Past smoker , %	878 (43.7)	189 (49.5)	0.044	44 (44.4)	0.970	130 (55.1)	0.001
Ever smoker , %	1661 (59.5)	355 (64.8)	0.024	90 (62.1)	0.600	227 (68.2)	0.003
Obesity (BMI ≥30 kg/m2), %	375 (13.4)	71 (13.0)	0.823	23 (16.0)	0.460	53 (15.9)	0.248
BMI, kg/m2	25.9 ± 3.8	25.8 ± 3.9	0.537	26.3 ± 3.9	0.303	26.4 ± 3.8	0.028
Central obesity, %	553 (19.8)	115 (21.0)	0.567	34 (23.4)	0.336	79 (23.7)	0.107
Waist circumference, cm	89.2 ± 11.9	88.7 ± 12.5	0.451	89.8 ± 12.0	0.529	90.7 ± 12.4	0.034
Metabolic syndrome, %	243 (8.7)	50 (9.1)	0.814	19 (13.1)	0.096	40 (12.0)	0.059

hs-CRP, mg/dL	0.1 [0.0 - 0.2]	0.1 [0.0 - 0.2]	0.480	0.1 [0.0 - 0.2]	0.514	0.1 [0.1 - 0.2]	0.027
GOT, U/L	18.0 [15.0 - 22.0]	18.0 [16.0 - 22.0]	0.394	18.0 [15.0 - 22.0]	0.502	19.0 [16.0 - 22.0]	0.289
GPT, U/L	20.0 [14.0 - 27.0]	18.0 [13.0 - 26.0]	0.041	19.0 [14.0 - 26.0]	0.832	20.0 [15.0 - 28.0]	0.662
GGT, U/L	20.0 [14.0 - 31.0]	20.0 [14.0 - 29.0]	0.491	21.7 [15.0 - 31.0]	0.366	22.9 [14.0 - 33.0]	0.078

Supplementary Table 4. No association between clonal hematopoiesis and blood pressure or glycated hemoglobin after adjustment for age and sex. The study population was stratified by the presence of any CH mutation, CH mutations with variant allele fraction (VAF) between 0.2-2% or ≥2%. P-values were obtained from logistic regression analysis adjusted for age and sex. Individuals taking antihypertensive or antidiabetic drugs were excluded from this analysis. SBP, systolic blood pressure; DBP, diastolic blood pressure; HbA1c, glycated hemoglobin.

	CH, any VAF			CH, VAF 0.2-2%			CH, VAF ≥2%		
	Estimate	**Std. Error**	**p-value**	**Estimate**	**Std. Error**	**p-value**	**Estimate**	**Std. Error**	**p-value**
SBP, mmHg	0.34	0.42	0.425	0.13	0.47	0.786	1.02	0.77	0.183
DBP, mmHg	0.40	0.34	0.241	0.34	0.38	0.373	0.55	0.63	0.380
HbA1c, %	0.02	0.01	0.114	0.02	0.02	0.239	0.04	0.03	0.164

Supplementary Table 5. No association between *DNMT3A*-mutant CH, *TET2*-mutant CH or other CH mutations with presence or extent of subclinical atherosclerosis, assessed cross-sectionally at baseline. CH status and subclinical atherosclerosis burden were determined at baseline. Presence of subclinical atherosclerosis was defined as a categorical variable based on CACS or 3DVUS imaging. The extent of subclinical atherosclerosis in those with detectable atherosclerosis in specific regions was defined as a continuous variable based on CACS or 3DVUS imaging. Statistical associations were evaluated using multivariate regression models adjusted for age and sex.

	DNMT3A mutations			*TET2* mutations			Other mutated genes		
Presence of atherosclerosis									
	OR	**95% CI**	**p-value**	**OR**	**95% CI**	**p-value**	**OR**	**95% CI**	**p-value**
CACs > 0	1.04	0.80 ; 1.34	0.771	1.26	0.81 ; 1.94	0.288	1.15	0.85 ; 1.54	0.36
Global plaque volume >0	0.91	0.74 ; 1.12	0.388	0.98	0.67 ; 1.41	0.898	1.05	0.81 ; 1.35	0.719
Carotid plaque volume >0	1.02	0.82 ; 1.26	0.855	1.13	0.77 ; 1.65	0.523	0.99	0.76 ; 1.28	0.936
Femoral plaque volume >0	0.92	0.74 ; 1.15	0.473	0.82	0.54 ; 1.22	0.328	1.1	0.85 ; 1.43	0.458
Extent of atherosclerosis									
	Estimate	**Std. Error**	**p-value**	**Estimate**	**Std. Error**	**p-value**	**Estimate**	**Std. Error**	**p-value**
CACS (Agatston)	14.1	20.02	0.481	-24.8	30.68	0.419	21.57	22.18	0.331
Global plaque volume (mm^3)	7.23	9.8	0.461	-26.1	16.39	0.112	-4.06	10.99	0.712
Carotid plaque volume (mm^3)	1.63	5.43	0.764	-16.28	9.13	0.075	1.25	6.54	0.849
Femoral plaque volume (mm^3)	5.6	11.14	0.615	-18.56	19.64	0.345	-7.3	12.05	0.545

Supplementary Table 6. Effects of clonal hematopoiesis (CH) on *de novo* femoral atherosclerosis development after adjustment for multiple hypothesis testing. This table provides Benjamini-Hochberg (BH) corrected p-values for the association between baseline CH mutations and the development of de novo femoral atherosclerosis over a 3-year follow-up period in the PESA study (related to Fig. 2e). Two distinct adjusted analyses are presented: one considering the different variables within each CH definition (i.e., CH, CHIP, or single gene analysis), and the other encompassing all CH variables used to assess the effect of CH on de novo femoral atherosclerosis development. BH, Benjamini-Hochberg.

	***De novo* femoral atherosclerosis development at the 3 year follow-up**		
CH variable	**Nominal p-value**	**BH-adjusted p-value (within each CH definition)**	**BH-adjusted p-value (all CH variables)**
CH	0.007	0.011	0.013
CH (VAF 0.2-2%)	0.072	0.072	0.081
CH (VAF ≥2%)	0.005	0.011	0.013
CHIP	0.006	0.009	0.013
CHIP (VAF 0.2-2%)	0.081	0.081	0.081
CHIP (VAF ≥2%)	0.003	0.009	0.013
DNMT3A mutations	0.025	0.038	0.038
TET2 mutations	0.045	0.045	0.058
Other mutated genes	0.004	0.012	0.013

Supplementary Table 7. Clonal hematopoiesis-related mutations identified longitudinally in the study population. Using deep targeted sequencing, we found 602 CH variants in 494 individuals from the PESA cohort both at baseline and at the 6-year follow-up. Ref. reference; Alt. Alternate; SNV, single nucleotide variant; VAF, variant allele fraction.

Please see Supplementary Table 7 spreadsheet.

Supplementary Table 8. Association between clonal hematopoiesis with different categories of variant allele fractions (VAF) and age. Statistical associations were evaluated using multivariate regression models.

VAF category	n	Estimate	Std.error	p-value
<0.2% (below threshold)	43	0.028	0.037	0.457
0.2-0.5%	305	0.06	0.015	3.64E-05
0.5-1%	337	0.093	0.014	4.33E-11
1-2%	282	0.085	0.015	1.12E-08
≥2%	248	0.111	0.016	1.86E-11

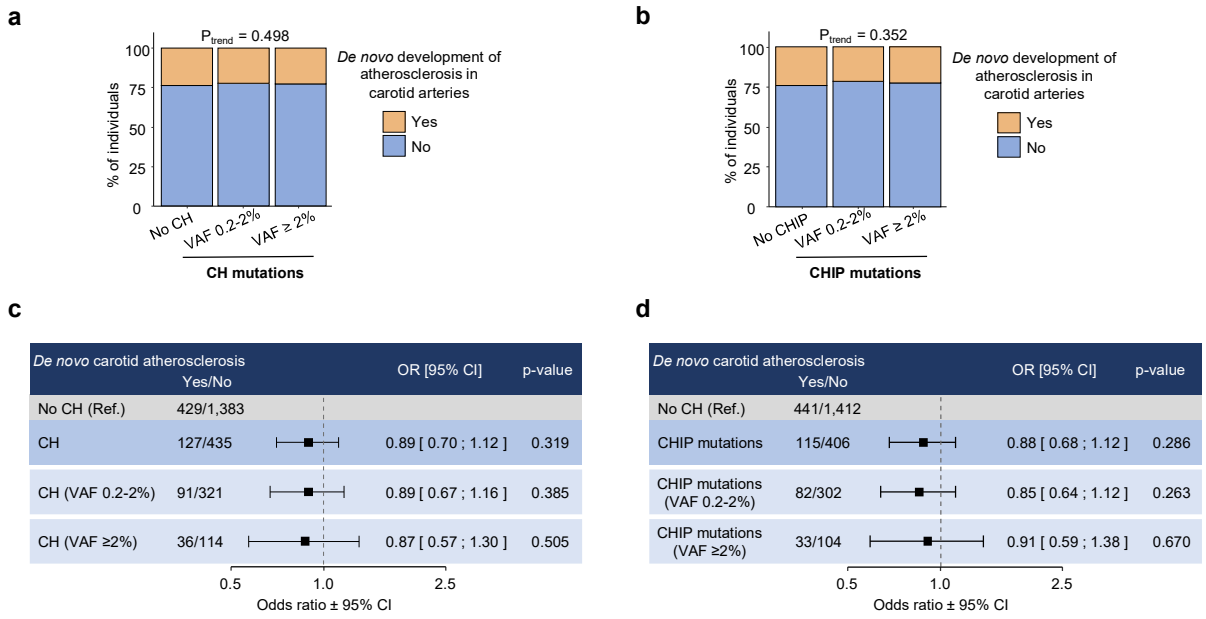

Supplementary Figure 1. Longitudinal assessment of the effects of clonal hematopoiesis (CH) on *de novo* carotid atherosclerosis development. We investigated the association between CH at baseline and *de novo* development of atherosclerosis in carotid arteries ~6-years after enrollment among PESA participants who initially lacked detectable atherosclerosis in this region. 3-dimensional-vascular ultrasound (3DVUS) imaging was used to determine the presence of carotid atherosclerosis. **a**, Incidence of *de novo* atherosclerosis development in carotid arteries in individuals free of CH (no CH) and in CH mutation carriers with VAF 0.2-2% or ≥ 2%. **b**, Incidence of *de novo* atherosclerosis development in carotid arteries in individuals free of myeloid CH (also termed CHIP), and in CHIP mutation carriers with VAF 0.2-2% or ≥ 2%. In **a** and **b**, statistical significance was evaluated using a univariate logistic regression analysis (n=2,374; p-value for trend is shown). **c**, Association between CH and *de novo* atherosclerosis development in carotid arteries. **d**, Association between mutations in myeloid genes (CHIP) and *de novo* atherosclerosis development in carotid arteries. In **c** and **d**, we used multivariate logistic regression models adjusted for age, sex, the cumulative effect of SBP, fasting glucose, LDL-C, BMI, smoking and lipid-lowering therapy status, and the cumulative systemic burden of atherosclerosis across the timeframe of the study (AUC for CACS, assessed by CT imaging, and global atherosclerotic plaque volume, assessed by 3DVUS imaging); bars indicate 95% confidence intervals centered in the mean value (square).

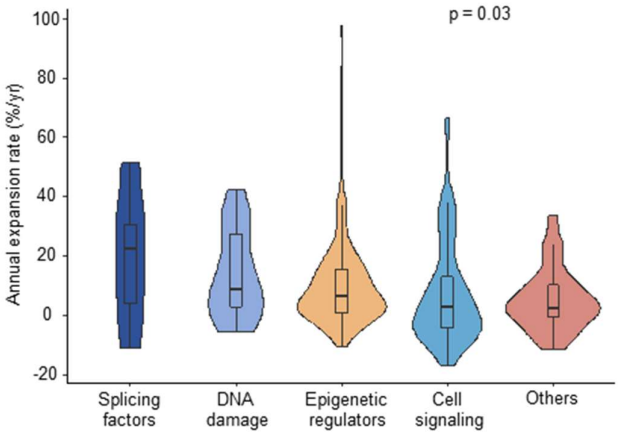

Supplementary Figure 2. Annual expansion rate (AER) of CH-related mutations classified by functional categories. Genes were grouped based on their biological function as epigenetic regulators (n=509 in *ASXL1, BCOR, BCORL1, DNMT3A, EZH2, IDH2, KDM6A, KMT2D, SETD2, SETDB1, SUZ12, TET2*), cell signaling regulators (n=38 in *CBL, GNAS, GNB1, JAK2, KRAS, MPL, MYD88, NRAS, STAT3, TNFAIP3*), DNA damage response genes (n=24 in *ATM, BRCC3, PPM1D, RAD21, TP53*), splicing factors (n=5 in *SF3B1, SRSF2, ZRSR2*) and other genes (n=26 in *BCL11B, CNOT3, NOTCH1, ZNF318*). Statistical significance was determined by Kruskal-Wallis test. Boxes represent the 25th (Q1), 50th (median) and 75th (Q3) percentiles of the data. The whiskers represent Q1 - 1.5*IQR at the minimum and Q3 + 1.5*IQR at the maximum.

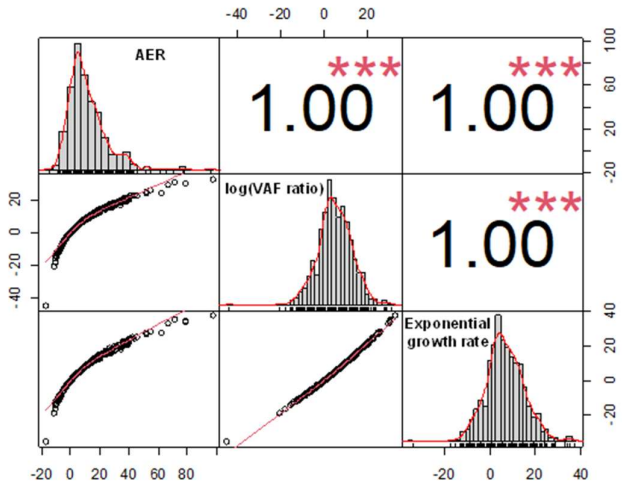

Supplementary Figure 3. Correlation matrix among alternative metrics for expansion rate of mutant hematopoietic clones. The diagonal shows the distribution of each variable. Below the diagonal are bivariate scatter plots with a fitted line. Above the diagonal, the Spearman's rank correlation coefficient values and p-values are indicated with stars (***, $p < 0.001$). AER, annual expansion rate. VAF, variant allelic fraction.